Vehicle Dynamic Model Assisted Inertial Navigation: Zero Velocity and Zero Turning Update

Oğuzhan ÇİFDALÖZ
Electrical–Electronics Eng.
Çankaya University
Ankara, Turkey
ocifdaloz@gmail.com

Yakup ÖZKAZANÇ
Electrical–Electronics Eng.
Hacettepe University
Ankara, Turkey
yakup.ozkazanc@gmail.com

Murat EREN
ASELSAN, Inc.
Ankara, Turkey
meren@aselsan.com.tr

Abstract

The objective of this paper is to present a method which aims to bound the error signals of an inertial navigation system (INS). Inertial navigation systems mainly utilize gyroscopes and accelerometers, and calculate velocity, position and attitude, essentially by integrating the measurements obtained from these sensors. Due to the nature of integration, INS are notoriously prone to sensor biases and drifts. Typically, GNSS are used to correct the navigation system errors caused by the inertial sensor measurements. However, in GNSS degraded or denied environments, alternative solutions are required. If the platform on which an INS is mounted is known or estimated to be stationary, zero-velocity update (ZUPT) and/or zero turning update (ZTUPT) algorithms can be applied to bound the navigation system errors. Under certain assumptions, ZUPT based algorithms can be applied when the platform is not stationary. If a vehicle's motion is constrained by the design of its kinematics, i.e. if it can be assumed that the vehicle cannot move or rotate along one or more of its body axes, ZUPT assisted Kalman estimators can be used to correct the errors along those axes. Potentially, ZUPT based estimation algorithms can also be utilized when a vehicle is performing specific types of maneuvers such as coordinated turns or level flight scenarios for aircraft or near constant velocity motion for other vehicles, especially if a specific variable is measured by another aiding sensor, or if a sufficiently high fidelity vehicle model is available. In this paper, the utilization of vehicle dynamics and kinematics is analyzed for the purpose of estimating navigation errors. The basic principle in vehicle model assisted navigation is based on combining the data produced by the vehicle model and the data obtained from the sensors onboard and the inertial navigation system through an Extended Kalman filter. Although model-assisted navigation requires additional software components, it potentially offers increased system accuracy and reliability. In vehicle dynamic model (VDM) assisted navigation, both the INS and VDM are valid at the same time and predict similar dynamic behavior, but contain different process and measurement noise. Incorporating the kinematics of the vehicle, along with a ZUPT and/or ZTUPT algorithm, provides additional data to feed into the Kalman filter and increases the efficiency of error estimation. Estimated error is then feedback into the INS algorithm.

I. Introduction

An inertial navigation system (INS) is comprised of an inertial measurement unit (IMU), assisting sensors and a sensor/data fusion algorithm. In the case where the assisting system is a global navigation satellite system (GNSS), an integrated INS/GNSS provides absolute position and attitude information. Other sensors and systems are required in order to bound the position, velocity and attitude errors of an INS when a GNSS is unavailable, denied or degraded due to jamming, disturbances, or physical conditions [1]. Accelerometers and gyroscopes in an IMU are subject to numerous error sources such as bias, scale factor, nonlinearities, dead zone, quantization, and bandwidth limitations. Since computing position, velocity and attitude is performed essentially by integrating the measurements obtained from these sensors, the navigation solution will diverge from the true solution. The objective of this study is to provide an extended Kalman filter based algorithm that can be utilized for the purpose of bounding navigation errors. Specifically, zero velocity update (ZUPT) and zero turning update (ZTUPT) methods

This research is funded by ASELSAN, Inc., Ankara, Turkey.

are investigated [2]. Hence, in this study, the vehicle is assumed to be stationary in a GNSS denied environment. Various methods are proposed to for zero velocity detection [3]–[5], and it is outside the scope of this study.

Navigation equations are highly nonlinear. They need to be linearized in order to implement an extended Kalman filter for state estimation. This is performed by approximating the nonlinear state equations, implemented both in Euler angles and quaternions, by a piece-wise constant system (PWCS) at each iteration. Approximating the nonlinear system at the current iteration's state-input combination helps capture the characteristic behavior of the system with little loss of accuracy [6], [7].

Through this implementation, expected outputs of a stationary (zero velocity and/or zero turning) vehicle and the outputs of the navigation equation are contrasted to obtain estimates of the navigation error states. In this sense, the control system is an output feedback controller. Error states are fed back to the navigation equations for the purposes of bounding INS errors, and simultaneously, estimating sensor drifts and biases.

The remainder of the paper is structured as follows: Section II states the problem to be addressed and describes the navigation system model, Section III describes the proposed solution and includes two scenarios, and finally Section IV summarizes the paper and presents future directions.

II. Problem Statement and Model

Inertial navigation systems utilize a variety of sensors such as gyroscopes, accelerometers, magnetometers, and compute velocity, position and attitude, essentially by integrating the measurements obtained from these sensors. Integration results in the problem of drifts in the solution, due to the biases and noise characteristics of these sensors. Typically, sensors which provide accurate position information are used in order to correct the navigation solution. A very common sensor is the GNSS. However, in environments where GNSS data are not available or degraded, alternative solutions are required.

In order to describe the method devised to bound inertial navigation errors, navigation equations that are used need to be described.

A. Navigation Equations

Navigation equations are nonlinear differential equations which define the position, velocity, and the attitude of the navigation system. They consist of three components: a set of equations to compute latitude, longitude, and altitue (L, λ, h), another set of equations to compute the north, east and down velocities in the navigation frame (v_N, v_E, v_D), and another set of equations to compute the roll, pitch and yaw Euler angles (ϕ, θ, ψ). If quaternions are used to compute the attitude of a system Euler angles are replaced by a rotation quaternion ($\mathbf{q} = [q_0\ q_1\ q_2\ q_3]^T$). Notation used throughout the document is due to [8].

Gyroscopes measure the angular rate of the body frame with respect to the inertial frame as resolved in the body frame and are given by

$$\omega_{ib}^{b} = \begin{bmatrix} \omega_x \\ \omega_y \\ \omega_z \end{bmatrix}$$

In order to compute the Euler angles, one needs the angular rate of the body frame with respect to the navigation frame as resolved in the body frame given as

$$\omega_{nb}^{b} = \omega_{ib}^{b} - C_n^b(\omega_{ie}^{n} + \omega_{en}^{n}) \tag{1}$$

where

$$\omega_{ie}^{n} = \begin{bmatrix} \Omega\cos L \\ 0 \\ -\Omega\sin L \end{bmatrix} \quad \text{and} \quad \omega_{en}^{n} = \begin{bmatrix} \dfrac{v_E}{R+h} \\ -\dfrac{v_N}{R+h} \\ -\dfrac{v_E\tan L}{R+h} \end{bmatrix} \tag{2}$$

are the turn rate of the earth and the transport rate, respectively. In Equations 1 and 2, R denotes the mean radius of the Earth, Ω denotes the turn rate of the Earth, and C_n^b denotes the transformation matrix from the navigation frame to the body frame.

The transformation matrix from the body frame to the navigation frame C_b^n is given by

$$C_b^n = (C_n^b)^T = \begin{bmatrix} \cos\psi\cos\theta & \cos\psi\sin\theta\sin\phi - \sin\psi\cos\phi & \cos\psi\sin\theta\cos\phi + \sin\psi\sin\phi \\ \sin\psi\cos\theta & \sin\psi\sin\theta\sin\phi + \cos\psi\cos\phi & \sin\psi\sin\theta\cos\phi - \cos\psi\sin\phi \\ -\sin\theta & \cos\theta\sin\phi & \cos\theta\cos\phi \end{bmatrix}$$

for Euler Angle implementation, and

$$C_b^n = (C_n^b)^T = \begin{bmatrix} q_0^2 + q_1^2 - q_2^2 - q_3^2 & 2q_1q_2 - 2q_0q_3 & 2q_0q_2 + 2q_1q_3 \\ 2q_0q_3 + 2q_1q_2 & q_0^2 - q_1^2 + q_2^2 - q_3^2 & 2q_2q_3 - 2q_0q_1 \\ 2q_1q_3 - 2q_0q_2 & 2q_0q_1 + 2q_2q_3 & q_0^2 - q_1^2 - q_2^2 + q_3^2 \end{bmatrix}$$

for quaternion implementation.

The first set of equations, so-called kinematic equation is used to compute the Euler angles or quaternions from gyroscope measurements, and is given by

$$\begin{bmatrix} \dot\phi \\ \dot\theta \\ \dot\psi \end{bmatrix} = \begin{bmatrix} 1 & \sin\phi\tan\theta & \cos\phi\tan\theta \\ 0 & \cos\phi & -\sin\phi \\ 0 & \sin\phi/\cos\theta & \cos\phi/\cos\theta \end{bmatrix} \omega_{nb}^b \tag{3}$$

for Euler angle implementation, and by

$$\begin{bmatrix} \dot q_0 \\ \dot q_1 \\ \dot q_2 \\ \dot q_3 \end{bmatrix} = \frac{1}{2}\begin{bmatrix} q_0 & -q_1 & -q_2 & -q_3 \\ q_1 & q_0 & -q_3 & q_2 \\ q_2 & q_3 & q_0 & -q_1 \\ q_3 & -q_2 & q_1 & q_0 \end{bmatrix} \begin{bmatrix} 0 \\ | \\ \omega_{nb}^b \\ | \end{bmatrix} = \frac{1}{2}\begin{bmatrix} 0 & -\omega_1 & -\omega_2 & -\omega_3 \\ \omega_1 & 0 & \omega_3 & -\omega_2 \\ \omega_2 & -\omega_3 & 0 & \omega_1 \\ \omega_3 & \omega_2 & -\omega_1 & 0 \end{bmatrix} \begin{bmatrix} q_0 \\ q_1 \\ q_2 \\ q_3 \end{bmatrix} \tag{4}$$

for quaternion implementation, where $[\omega_1 \;\; \omega_2 \;\; \omega_3]^T \triangleq \omega_{nb}^b$.

The second set of navigation equations are associated with the North, East, Down velocities of the navigation system, given by

$$\begin{bmatrix} \dot v_N \\ \dot v_E \\ \dot v_D \end{bmatrix} = \mathbf{C}_b^n \mathbf{f}^b - (2\omega_{ie}^n + \omega_{en}^n) \times \begin{bmatrix} v_N \\ v_E \\ v_D \end{bmatrix} + \begin{bmatrix} 0 \\ 0 \\ g(h) \end{bmatrix} \tag{5}$$

where, assuming a spherical earth,

$$g(h) = \frac{g_0}{\left(1 + \frac{h}{R}\right)^2}.$$

In Equation 5, g_0 denotes the gravitational acceleration of the Earth and $\mathbf{f}^b$ denotes the accelerometer measurements, i.e.

$$\mathbf{f}^b = \begin{bmatrix} f_x \\ f_y \\ f_z \end{bmatrix}$$

The third set of navigation equations are associated with the geographic coordinates and altitude. It is given by

$$\begin{bmatrix} \dot{L} \\ \dot{\lambda} \\ \dot{h} \end{bmatrix} = \begin{bmatrix} \frac{1}{R+h} & 0 & 0 \\ 0 & \frac{\sec L}{R+h} & 0 \\ 0 & 0 & -1 \end{bmatrix} \begin{bmatrix} v_N \\ v_E \\ v_D \end{bmatrix} \tag{6}$$

Equations 3/4, 5, and 6 can be combined to form a first order non-linear differential equation to represent the navigation equations as

$$\dot{x} = f(x(t), u(t)), \qquad x(t_o) = x_o \tag{7}$$

where

$$x(t) = [L(t) \;\; \lambda(t) \;\; h(t) \;\; v_N(t) \;\; v_E(t) \;\; v_D(t) \;\; \phi(t) \;\; \theta(t) \;\; \psi(t)]^T$$

for Euler angle implementation,

$$x(t) = [L(t) \;\; \lambda(t) \;\; h(t) \;\; v_N(t) \;\; v_E(t) \;\; v_D(t) \;\; q_0(t) \;\; q_1(t) \;\; q_2(t) \;\; q_3(t)]^T$$

for quaternion implementation, and the inputs are the sensor measurements, i.e.,

$$u(t) = [f_x(t) \;\; f_y(t) \;\; f_z(t) \;\; \omega_x(t) \;\; \omega_y(t) \;\; \omega_z(t)]^T$$

B. Linear Navigation Equations

A linear state space representation which approximates a nonlinear system

$$\dot{x} = f(x(t), u(t))$$
$$y = g(x(t), u(t))$$

about a fixed point (x_*, u_*) is obtained as follows. For

$$\delta x(t) \triangleq x(t) - x_* \qquad \text{and} \qquad \delta u(t) \triangleq u(t) - u_*$$

$$\delta \dot{x}(t) = \mathbf{A}\delta x(t) + \mathbf{B}\delta u(t) \tag{8}$$
$$y(t) = \mathbf{C}\delta x(t) + \mathbf{D}\delta u(t) \tag{9}$$

where

$$\mathbf{A} = \left.\frac{\partial f(x,u)}{\partial x}\right|_{(x_*,u_*)} \triangleq \left[\begin{matrix} \frac{\partial f_1}{\partial x_1} & \cdots & \frac{\partial f_1}{\partial x_n} \\ \vdots & \ddots & \vdots \\ \frac{\partial f_n}{\partial x_1} & \cdots & \frac{\partial f_n}{\partial x_n} \end{matrix}\right]_{(x_*,u_*)}, \quad \mathbf{B} = \left.\frac{\partial f(x,u)}{\partial u}\right|_{(x_*,u_*)} \triangleq \left[\begin{matrix} \frac{\partial f_1}{\partial u_1} & \cdots & \frac{\partial f_1}{\partial u_m} \\ \vdots & \ddots & \vdots \\ \frac{\partial f_n}{\partial u_1} & \cdots & \frac{\partial f_n}{\partial u_m} \end{matrix}\right]_{(x_*,u_*)}$$

$$\mathbf{C} = \left.\frac{\partial g(x,u)}{\partial x}\right|_{(x_*,u_*)}, \quad \mathbf{D} = \left.\frac{\partial g(x,u)}{\partial u}\right|_{(x_*,u_*)}$$

For the system given in 7 when $h_{eq} = \phi_{eq} = \theta_{eq} = \psi_{eq} = 0$, the Euler angle implementation yields

$$A = \begin{bmatrix} | & | & | \\ A_1 & A_2 & A_3 \\ | & | & | \end{bmatrix} \tag{10}$$

where

$$A_1 = \begin{bmatrix} 0 & 0 & -\frac{v_N}{R^2} \\ \frac{v_E \tan L}{R \cos L} & 0 & -\frac{v_E}{R^2 \cos L} \\ 0 & 0 & 0 \\ -v_E \left(2\Omega \cos L + \frac{v_E}{R \cos^2 L}\right) & 0 & \frac{v_E^2 \tan L - v_D v_N}{R^2} \\ 2\Omega(v_N \cos L - v_D \sin L) + \frac{v_N v_E}{R \cos^2 L} & 0 & -\frac{v_E(v_D + v_N \tan L)}{R^2} \\ 2\Omega v_E \sin L & 0 & \frac{v_E^2 + v_N^2 - 2g_0 R}{R^2} \\ \Omega \sin L & 0 & \frac{v_E}{R^2} \\ 0 & 0 & -\frac{v_N}{R^2} \\ \Omega \cos L + \frac{v_E}{R \cos^2 L} & 0 & -\frac{v_E \tan L}{R^2} \end{bmatrix}$$

$$A_2 = \begin{bmatrix} \frac{1}{R} & 0 & 0 \\ 0 & \frac{1}{R \cos L} & 0 \\ 0 & 0 & -1 \\ \frac{v_D}{R} & -2\Omega \sin L - \frac{2v_E \tan L}{R} & \frac{v_N}{R} \\ 2\Omega \sin L + \frac{v_E \tan L}{R} & \frac{v_D + v_N \tan L}{R} & 2\Omega \cos L + \frac{v_E}{R} \\ -\frac{2v_N}{R} & -2\Omega \cos L - \frac{2v_E}{R} & 0 \\ 0 & -\frac{1}{R} & 0 \\ \frac{1}{R} & 0 & 0 \\ 0 & \frac{\tan L}{R} & 0 \end{bmatrix}$$

$$A_3 = \begin{bmatrix} 0 & 0 & 0 \\ 0 & 0 & 0 \\ 0 & 0 & 0 \\ 0 & f_z & -f_y \\ -f_z & 0 & f_x \\ f_y & -f_x & 0 \\ 0 & \omega_z & \frac{v_N}{R} \\ -\omega_z & 0 & \Omega \cos L + \frac{v_E}{R} \\ \omega_y & -\Omega \cos L - \frac{v_E}{R} & 0 \end{bmatrix}$$

and

$$B = \begin{bmatrix} \mathbf{0}_{3\times3} & \mathbf{0}_{3\times3} \\ \hat{C}_b^m & \mathbf{0}_{3\times3} \\ \mathbf{0}_{3\times3} & \hat{T} \end{bmatrix} \tag{11}$$

where

$$\hat{C}_b^m = \begin{bmatrix} \cos\psi_{eq}\cos\theta_{eq} & \cos\psi_{eq}\sin\theta_{eq}\sin\phi_{eq} - \sin\psi_{eq}\cos\phi_{eq} & \cos\psi_{eq}\sin\theta_{eq}\cos\phi_{eq} + \sin\psi_{eq}\sin\phi_{eq} \\ \sin\psi_{eq}\cos\theta_{eq} & \sin\psi_{eq}\sin\theta_{eq}\sin\phi_{eq} + \cos\psi_{eq}\cos\phi_{eq} & \sin\psi_{eq}\sin\theta_{eq}\cos\phi_{eq} - \cos\psi_{eq}\sin\phi_{eq} \\ -\sin\theta_{eq} & \cos\theta_{eq}\sin\phi_{eq} & \cos\theta_{eq}\cos\phi_{eq} \end{bmatrix}$$

and

$$\hat{T} = \begin{bmatrix} 1 & \sin\phi_{eq}\tan\theta_{eq} & \cos\phi_{eq}\tan\theta_{eq} \\ 0 & \cos\phi_{eq} & -\sin\phi_{eq} \\ 0 & \sin\phi_{eq}/\cos\theta_{eq} & \cos\phi_{eq}/\cos\theta_{eq} \end{bmatrix}$$

Note that the B matrix is given for any Euler angle and altitude combination. (i.e. $h_{eq}, \phi_{eq}, \theta_{eq}, \psi_{eq}$ are not necessarily zero.)

III. Proposed Solution and Results

Figure 1 outlines the structure of the algorithm devised to bound the navigation errors of an INS. In Figure 1,

- $u \triangleq [f_x \ f_y \ f_z \ \omega_x \ \omega_y \ \omega_z]^T$ denotes the IMU measurements,
- $x \triangleq [L \ \lambda \ h \ v_N \ v_E \ v_D \ \phi \ \theta \ \psi]^T$ denotes the navigation states,
- $g(x)$ denotes the output function,
- y denotes the output,
- $\tilde{y}$ denotes the outputs of an assisting sensor or the output of a vehicle model,
- u_c denotes the state correction signal, and
- K denotes the extended Kalman filter algorithm.

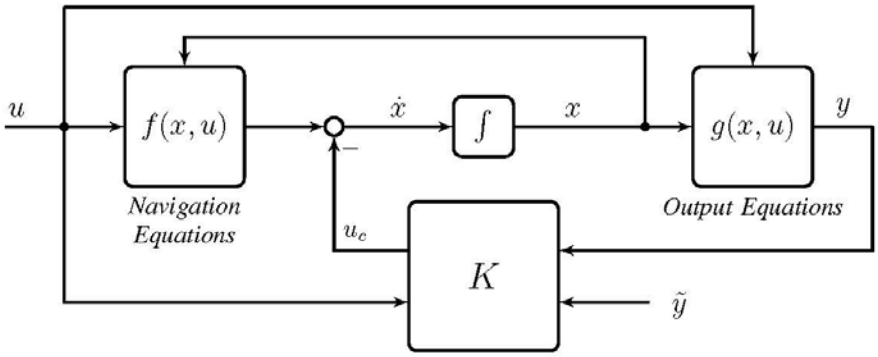

Fig. 1: Control System Structure

K is obtained via solving an Algebraic Riccati Equation based on the linearized dynamics of $f(x,u)$, and the covariance matrices associated with process and measurement noise.

In this study, the Extended Kalman filter is implemented in discrete time. ZOH discretization of the equations given in 8 and 9 at a sampling period of T_s are

$$x_{k+1} = \mathbf{F}_k x_k + \mathbf{G}_k u_k$$
$$y_k = \mathbf{H}_k x_k + \mathbf{N}_k u_k$$

where

$$exp\left\{\begin{bmatrix} \mathbf{A} & \mathbf{B} \\ 0 & 0 \end{bmatrix} T_s\right\} = \begin{bmatrix} \mathbf{F}_k & \mathbf{G}_k \\ 0 & \mathbf{I} \end{bmatrix}, \qquad \mathbf{H}_k = \mathbf{C}, \qquad and \qquad \mathbf{N}_k = \mathbf{D}.$$

In systems where high precision inertial sensors are used, inertial sensor errors are also added to the state vector, resulting in a more detailed navigation model. After linearization about a fixed (x_k, u_k)

$$\begin{bmatrix} x_{k+1} \\ b_{k+1} \end{bmatrix} = \begin{bmatrix} \mathbf{F}_k & \mathbf{G}_k \\ 0 & \mathbf{I} \end{bmatrix} \begin{bmatrix} x_k \\ b_k \end{bmatrix} + \begin{bmatrix} \mathbf{G}_k \\ 0 \end{bmatrix} u_k \tag{12}$$

$$y_k = \begin{bmatrix} \mathbf{H}_k & 0 \end{bmatrix} \begin{bmatrix} x_k \\ b_k \end{bmatrix} + \mathbf{H}_k u_k \tag{13}$$

is obtained where b_k denotes the sampled inertial sensor errors.

Finally, an extended Kalman filter can be implemented [9]. At each step, a Kalman gain, K, is computed and by

$$u_c = K(y - \tilde{y})$$

loop is closed as shown in Figure 1.

In the following subsections, ZUPT and ZTUPT algorithms are demonstrated on selected scenarios.

A. Zero Velocity Update (ZUPT)

Assume a land vehicle such that

$$\begin{bmatrix} L \\ \lambda \\ h \end{bmatrix} = \begin{bmatrix} L_o \\ \lambda_o \\ h_o \end{bmatrix}, \qquad \begin{bmatrix} v_N \\ v_E \\ v_D \end{bmatrix} = \begin{bmatrix} 0 \\ 0 \\ 0 \end{bmatrix} \qquad \text{and} \qquad \begin{bmatrix} \phi \\ \theta \\ \psi \end{bmatrix} = \begin{bmatrix} \phi_o \\ \theta_o \\ \psi_o \end{bmatrix}$$

where $(\cdot)_o$ take fixed values depending on the vehicle's location of the vehicle on Earth. ZUPT algorithm assumes no knowledge of the orientation of the vehicle. Hence,

$$\tilde{y} = [L \;\; \lambda \;\; h \;\; v_N \;\; v_E \;\; v_D]^T$$

Given the above and using Equations 1 and 5 ideal sensor measurements can be computed as

$$\begin{bmatrix} f_x \\ f_y \\ f_z \end{bmatrix} = \begin{bmatrix} -g\sin\theta \\ g\cos\theta\sin\phi \\ g\cos\theta\cos\phi \end{bmatrix} = \begin{bmatrix} 0 \\ 0 \\ -g \end{bmatrix} \qquad \text{and} \qquad \begin{bmatrix} \omega_x \\ \omega_y \\ \omega_z \end{bmatrix} = C_n^b \begin{bmatrix} \Omega\cos L \\ 0 \\ -\Omega\sin L \end{bmatrix}$$

Figures on the left include the results when the extended Kalman filter is not functional. In other words left figures show what values the state would take if left alone. Figures on the right present the result when the filter is functional.

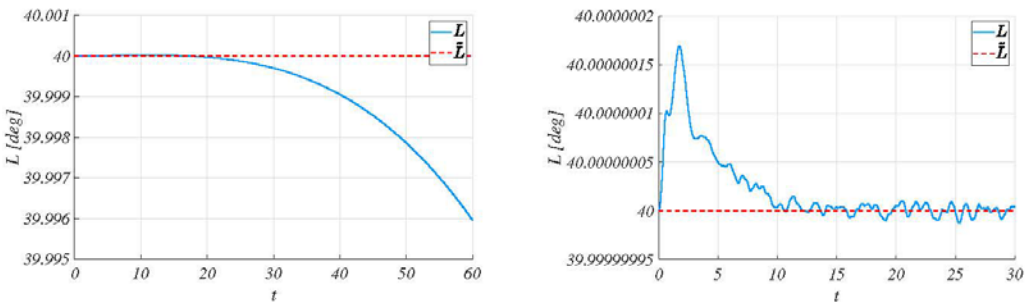

(a) Filter OFF (b) Filter ON

Fig. 2: Latitude

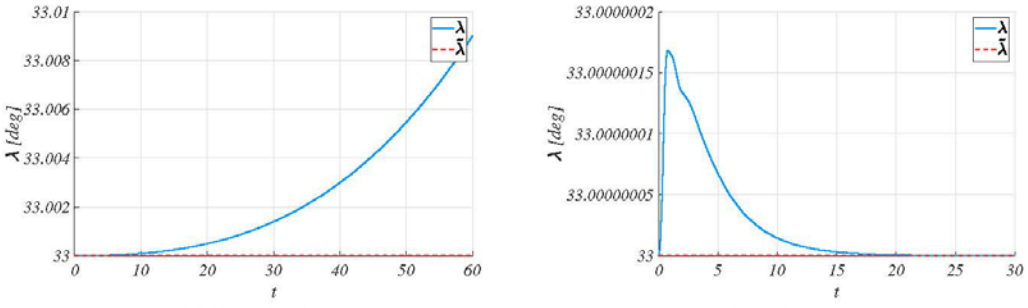

(a) Filter OFF (b) Filter ON

Fig. 3: Longitude

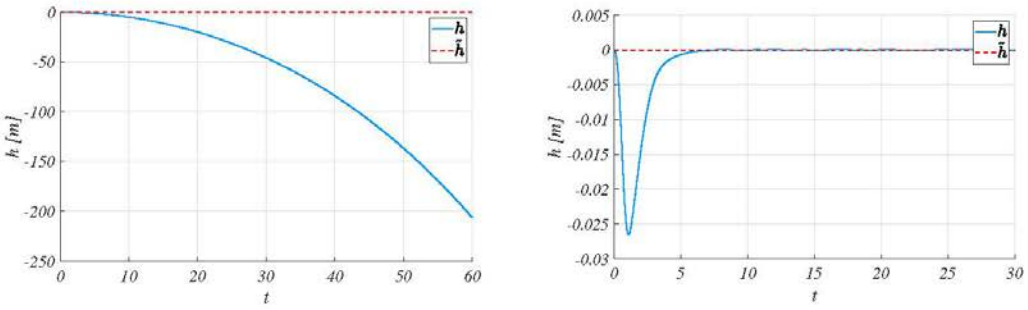

(a) Filter OFF (b) Filter ON

Fig. 4: Altitude

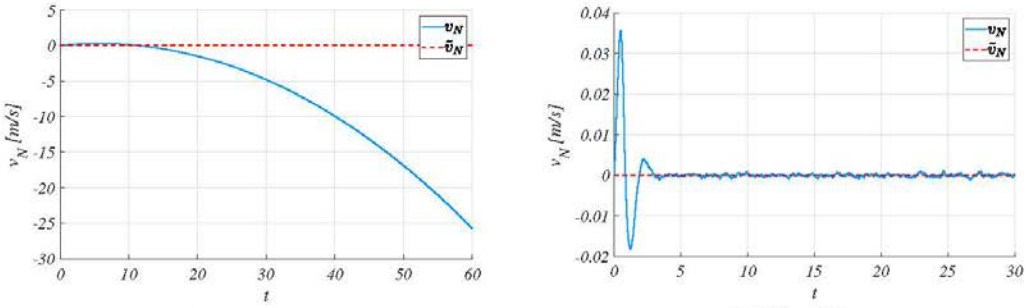

(a) Filter OFF (b) Filter ON

Fig. 5: North Velocity

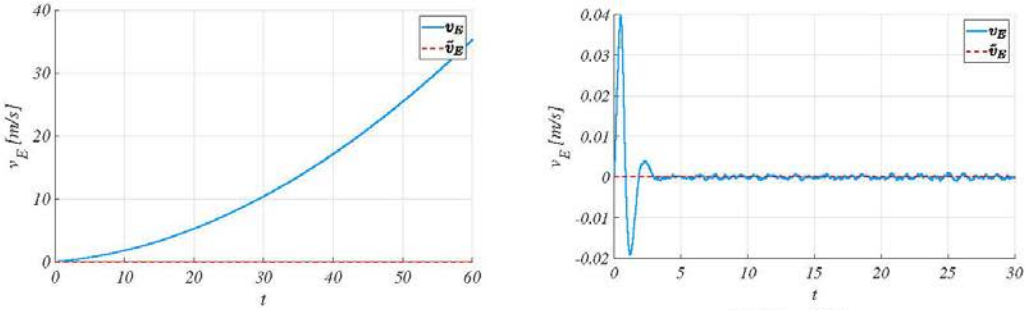

(a) Filter OFF (b) Filter ON

Fig. 6: East Velocity

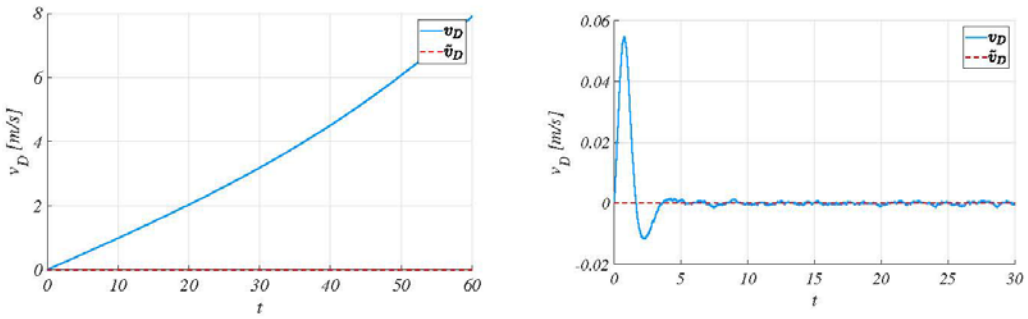

(a) Filter OFF (b) Filter ON

Fig. 7: Down Velocity

Figures 2 – 7 show that the method is performing as expected at steady state. Note that the positions, and (zero) velocities are available to the filter as outputs. Latitude, longitude, and altitude maintain their initial conditions. North, east, and down velocities are enforced to remain at zero.

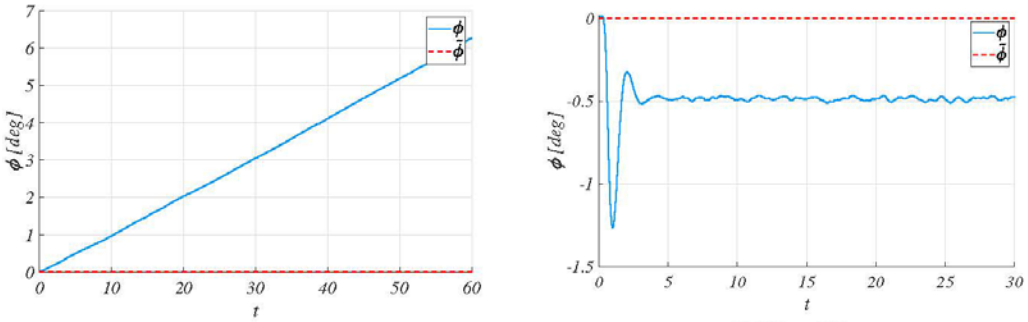

(a) Filter OFF (b) Filter ON

Fig. 8: Roll Angle

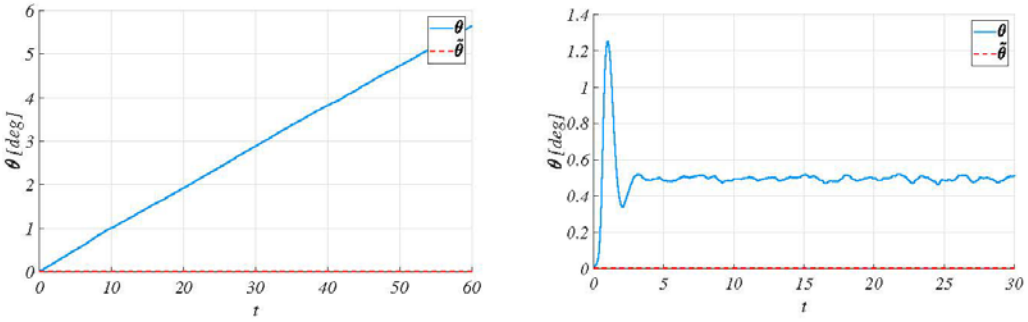

(a) Filter OFF (b) Filter ON

Fig. 9: Pitch Angle

Figures 8 and 9 demonstrate that the ZUPT algorithm also bounds roll and and pitch angle errors, although it cannot drive them to zero.

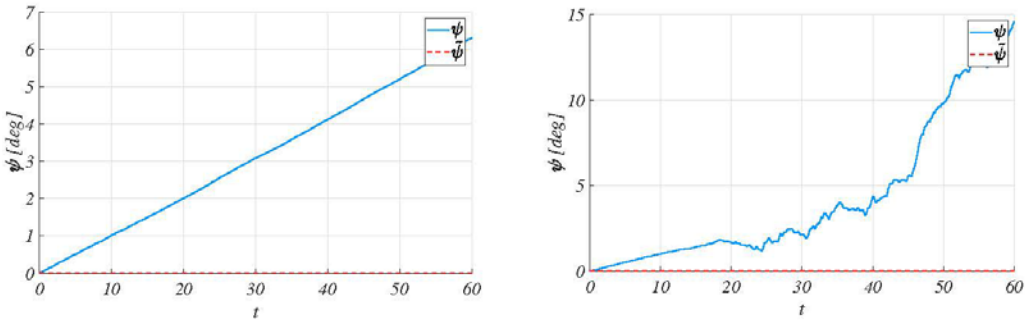

(a) Filter OFF (b) Filter ON

Fig. 10: Heading Angle

Figures 10 shows that the ZUPT algorithm has no impact on the heading angle.The main reason behind this result is the fact that the heading angle is an unobservable state. (It performed even worse than the nonfunctional filter scenario, although this is completely due to the random sensor noise generated in the simulation. In other simulation runs, functional filter scenario could be better.)

B. Zero Turning Update (ZTUPT)

The main premise of ZTUPT is to feed into the Kalman filter the additional information that a vehicle at rest is also non-rotating, i.e. its Euler angle rates are zero. Euler rates evolve in time in accordance with

$$\begin{bmatrix} \dot{\phi} \\ \dot{\theta} \\ \dot{\psi} \end{bmatrix} = T_{euler}(\omega_{ib}^b - C_n^b(\omega_{ie}^n + \omega_{en}^n)) \tag{14}$$

where

$$T_{euler} = \begin{bmatrix} 1 & \sin\phi\tan\theta & \cos\phi\tan\theta \\ 0 & \cos\phi & -\sin\phi \\ 0 & \sin\phi/\cos\theta & \cos\phi/\cos\theta \end{bmatrix}$$

ZTUPT is applicable when

$$\begin{bmatrix} \dot{\phi} \\ \dot{\theta} \\ \dot{\psi} \end{bmatrix} = 0 \tag{15}$$

For Equation 14 to be equal to zero, either $T_{euler} = 0$, or it has a non-empty null space, or $\omega_{ib}^b - C_n^b(\omega_{ie}^n + \omega_{en}^n) = 0$. It can be shown that the right null space of T_{euler} is empty and it is never equal to 0. Hence, it must be that

$$\omega_{nb}^b = \omega_{ib}^b - C_n^b(\omega_{ie}^n + \omega_{en}^n) = 0$$

However, since a vehicle at rest has zero linear velocities as well, the above equation further simplifies to

$$\omega_{ib}^b - C_n^b\omega_{ie}^n = 0 \tag{16}$$

which describes what the sensors should measure under such zero velocity and turning conditions.

ZTUPT is implemented by augmenting the navigation output equation, $g(x,u)$, by Equation 15 and incorporating it in the extended filter. Please note that Equation 15 can be defined as a function of the system states.

Assume a land vehicle such that

$$\begin{bmatrix} L \\ \lambda \\ h \end{bmatrix} = \begin{bmatrix} L_o \\ \lambda_o \\ h_o \end{bmatrix}, \qquad \begin{bmatrix} v_N \\ v_E \\ v_D \end{bmatrix} = \begin{bmatrix} 0 \\ 0 \\ 0 \end{bmatrix} \qquad \text{and} \qquad \begin{bmatrix} \phi \\ \theta \\ \psi \end{bmatrix} = \begin{bmatrix} \phi_o \\ \theta_o \\ \psi_o \end{bmatrix}$$

where $(\cdot)_o$ take fixed values depending on the vehicle's location of the vehicle on Earth. ZTUPT algorithm assumes no knowledge of the orientation of the vehicle. Hence,

$$\tilde{y} = [L \;\; \lambda \;\; h \;\; v_N \;\; v_E \;\; v_D \;\; \dot{\phi} \;\; \dot{\theta} \;\; \dot{\psi}]^T$$

The last three states correspond to the augmented zero turn states.

Given the above and using Equations 1 and 5 ideal sensor measurements can be computed as

$$\begin{bmatrix} f_x \\ f_y \\ f_z \end{bmatrix} = \begin{bmatrix} -g\sin\theta \\ g\cos\theta\sin\phi \\ g\cos\theta\cos\phi \end{bmatrix} \qquad \text{and} \qquad \begin{bmatrix} \omega_x \\ \omega_y \\ \omega_z \end{bmatrix} = C_n^b \begin{bmatrix} \Omega\cos L \\ 0 \\ -\Omega\sin L \end{bmatrix}$$

In the following example, it was also assumed that when the ZTUPT is activated, there is a 500m of altitude error accumulated in the navigation system.

As before, Figures on the left include the results when the extended Kalman filter is not functional, Figures on the right present the result when the filter is functional.

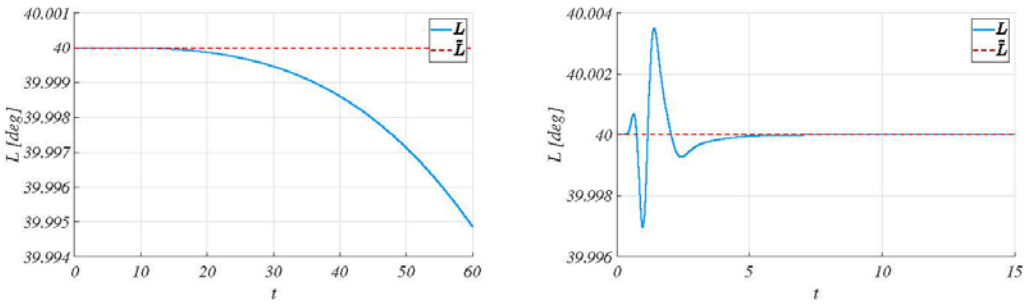

(a) Filter OFF (b) Filter ON

Fig. 11: Latitude

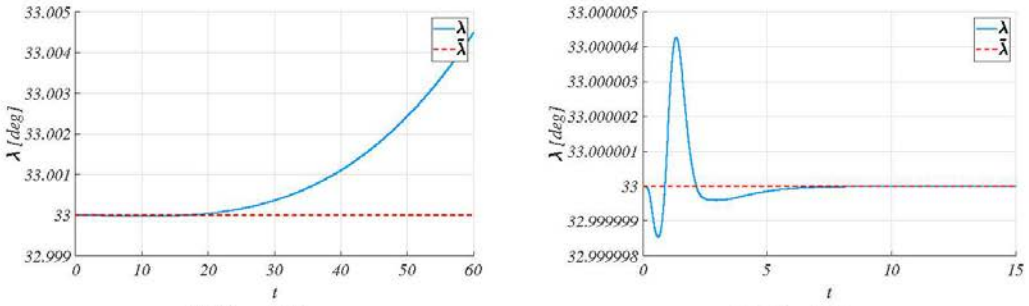

(a) Filter OFF (b) Filter ON

Fig. 12: Longitude

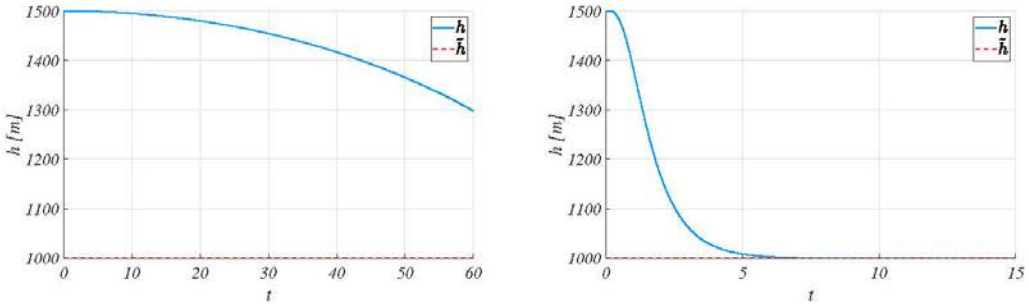

(a) Filter OFF (b) Filter ON

Fig. 13: Altitude

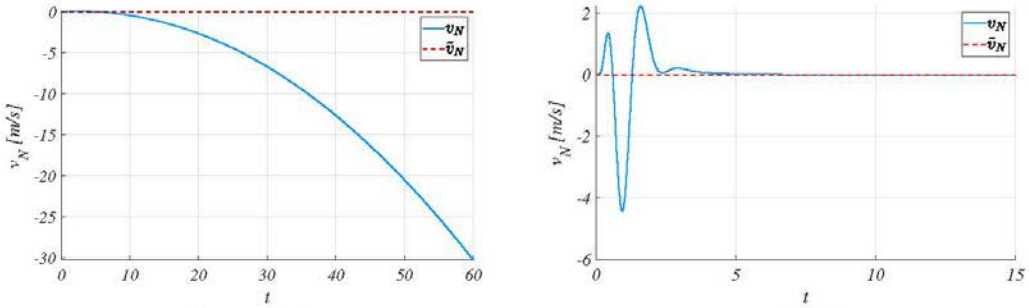

(a) Filter OFF (b) Filter ON

Fig. 14: North Velocity

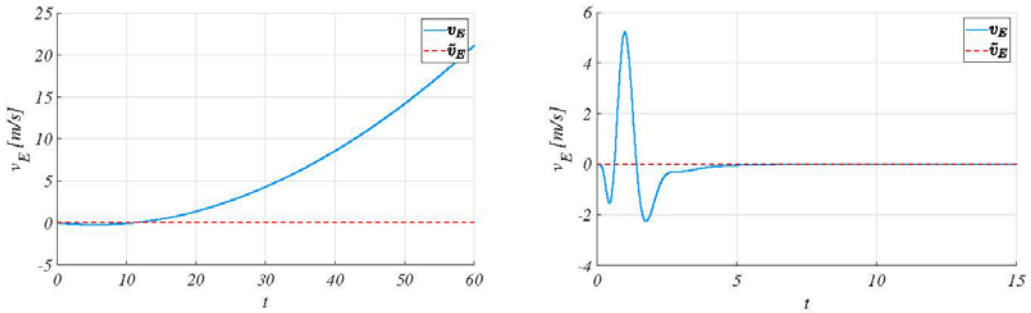

(a) Filter OFF (b) Filter ON

Fig. 15: East Velocity

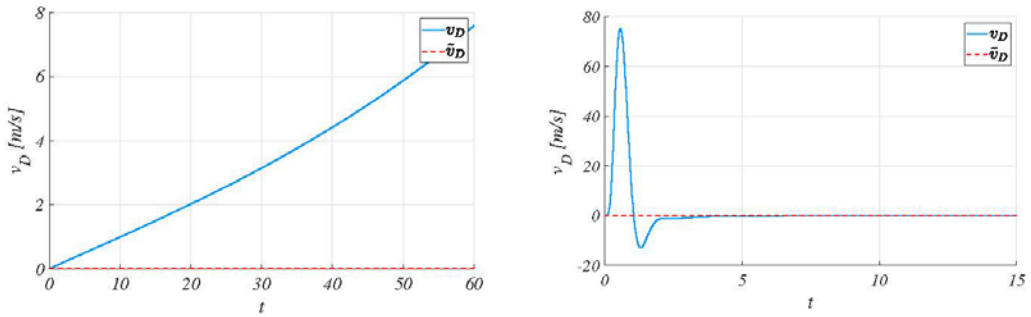

(a) Filter OFF (b) Filter ON

Fig. 16: Down Velocity

Figures 11 – 16 show that the method is performing as expected at steady state. Note that the positions, and (zero) velocities are available to the filter as outputs. Latitude and longitude maintain their initial conditions. Altitude converges to the true altitude. North, east, and down velocities are enforced to remain at zero.

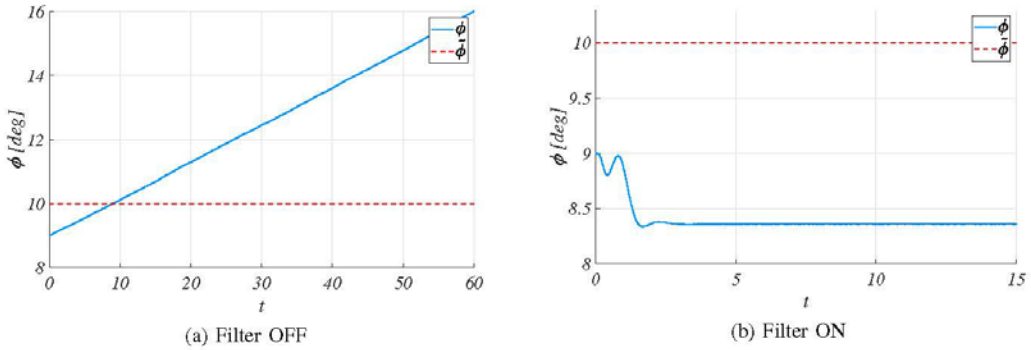

(a) Filter OFF (b) Filter ON

Fig. 17: Roll Angle

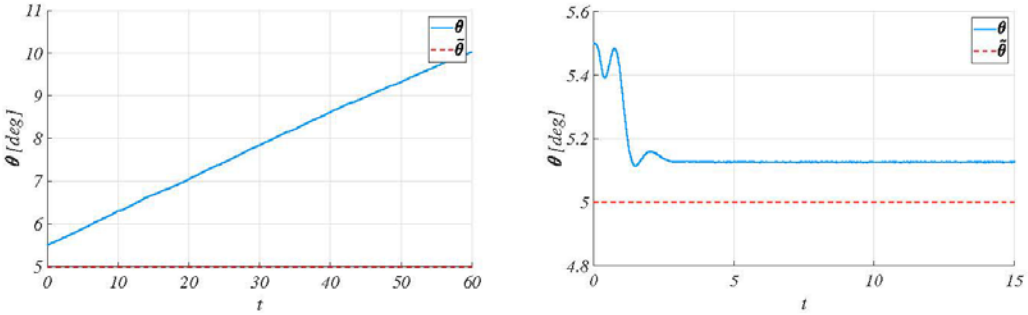

(a) Filter OFF (b) Filter ON

Fig. 18: Pitch Angle

Figures 17 and 18 demonstrate that the ZTUPT algorithm also bounds roll and and pitch angle errors, although it cannot drive them to zero.

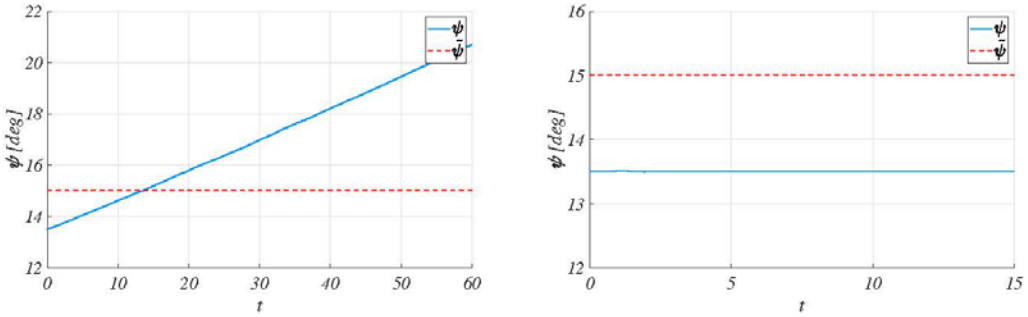

(a) Filter OFF (b) Filter ON

Fig. 19: Heading Angle

Figures 19 shows one of the expected benefits of the ZTUPT. Although it cannot be driven to its true value, heading angle errors are also bounded by the ZTUPT. We say that this is expected because ZTUPT specifically "tells" the control system that the system is not rotating.

IV. Summary and Future Work

This study should be considered as a first step towards utilizing vehicle dynamics as an aiding algorithm to an inertial navigation system. Although, in this paper, a dynamic model is not introduced, properties of a non-moving vehicle is utilized. Reducing navigation errors while at rest is challenging because of the observability issues associated with the linearized dynamics of the system. Additionally, at rest, some of the sensors do measure zero, which makes estimation even harder. In this study two methods, ZUPT and ZTUPT, are discussed and simulation results are presented. ZUPT manages to bound the navigation errors except for the heading angle. As a matter of fact, ZUPT has no effect on the heading angle. ZTUPT performed better that ZUPT overall, and also managed to bound heading angle errors. Both methods, as expected, failed to drive the attitude states to zero. Future work is going to try to incorporate a vehicle dynamical model into the extended Kalman filter structure and investigate the possibility of bounding navigation errors via an implementable framework.

REFERENCES

[1] G. T. Schmidt, "Navigation sensors and systems in GNSS degraded and denied environments," in Chinese Journal of Aeronautics, vol. 28, pp. 1–10, 2015.
[2] Y. Akcayir and Y. Ozkazanc, "Gyroscope drift estimation analysis in land navigation systems," Proceedings of 2003 IEEE Conference on Control Applications, vol.2, pp. 1488–1491, 2003.
[3] J. Wahlström, I. Skog, F. Gustafsson, A. Markham and N. Trigoni, "Zero-Velocity Detection—A Bayesian Approach to Adaptive Thresholding," in IEEE Sensors Letters, vol. 3, no. 6, pp. 1–4, 2019.
[4] L. Xiaofang, M. Yuliang, X. Ling, C. Jiabin and S. Chunlei, "Applications of zero-velocity detector and Kalman filter in zero velocity update for inertial navigation system," Proceedings of 2014 IEEE Chinese Guidance, Navigation and Control Conference, pp. 1760–1763, 2014.
[5] B. Wagstaff and J. Kelly, "LSTM-Based Zero-Velocity Detection for Robust Inertial Navigation," in International Conference on Indoor Positioning and Indoor Navigation, pp. 1-8, 2018.
[6] D. Goshen-Meskin and I. Y. Bar-Itzhack, "Observability analysis of piece-wise constant systems. I. Theory," in IEEE Transactions on Aerospace and Electronic Systems, vol. 28, no. 4, pp. 1056-1067, 1992.
[7] D. Goshen-Meskin and I. Y. Bar-Itzhack, "Observability analysis of piece-wise constant systems. II. Application to inertial navigation in-flight alignment (military applications)," in IEEE Transactions on Aerospace and Electronic Systems, vol. 28, no. 4, pp. 1068–1075, 1992.
[8] D. Titterton and J. Weston, "Strapdown inertial navigation technology." The American Institute of Aeronautics and Astronautics, second ed., 2004.
[9] H.Ma, L. Yan, Y. Xia and M. Fu, "Kalman Filtering and Information Fusion." Science Press, 2020.